Turkish Journal of Remote Sensing and GIS
Türk Uzaktan Algılama ve CBS Dergisi

Turk J Remote Sens GIS, March 2023, 4(1): 83-99
Journal homepage: http://www.dergipark.org.tr/en/pub/rsgis

Effect of Camera Calibration Refreshing on Orthophoto Position Accuracy in UAV Mapping

İHA'larda Kamera Kalibrasyonun Ortofoto Konum Doğruluğuna Etkisi

Cumhur Şahin[1]*

[1]Gebze Technical University, Faculty of Engineering, Department of Geomatics Engineering, 41400, Gebze, Kocaeli/Türkiye.

ORIGINAL PAPER

***Corresponding author:**
Cumhur Şahin
csahin@gtu.edu.tr

doi: 10.48123/rsgis.1207512

Article history
Received: 20.11.2022
Accepted: 20.02.2023
Published: 28.03.2023

Abstract

Unmanned aerial vehicles (UAVs) are autonomous or remote control controlled air vehicles without a pilot. UAVs are aerial platforms capable of carrying non-metric photogrammetric equipment. In this study; the effect of two different calibration values of the camera available on the DJI Phantom 4 Pro equipment to the ortho-photo maps obtained from two different flight heights was investigated. An area within the campus of Gebze Technical University was chosen as a study area. PI 3000 software was used to calibrate the camera and the differences between the calculated parameters and the conventional parameters were determined. Also, the effect of the parameters on position accuracy was investigated. In the photogrammetric stereo model, the rms of Z depends on the picture scale, flight height, base length and the measurement accuracy of image coordinates. Since the measurement accuracy of the image coordinates x, y is also affected by the calibration accuracy, the calibration field independent of the Z value can be used. Geo-referencing and field measurements of the orthophotos produced by the GPS and measurement of the work area from two different heights with UAVs. Office work is the part where orthophotos are produced, georeferenced and analyzed with GPS coordinates of control points. The data obtained in the study reduces the rms value when recalibration is performed at a low flight altitude. However, a similar result could not be obtained for 120 meters flight altitude.

Keywords: *UAV, Photogrammetry, Camera calibration, Orthophoto*

Özet

İnsansız hava araçları (İHA), pilotsuz otonom veya uzaktan kumandalı hava araçlarıdır. İHA'lar, metrik olmayan fotogrametrik ekipman taşıyabilen hava platformlarıdır. Bu çalışmada; DJI Phantom 4 Pro ekipmanı üzerinde bulunan kameranın iki farklı kalibrasyon değerinin iki farklı uçuş yüksekliğinden elde edilen ortofoto haritalara etkisi araştırılmıştır. Çalışma alanı olarak Gebze Teknik Üniversitesi kampüsü içerisinde bir alan seçilmiştir. Kameranın kalibrasyonu için PI 3000 yazılımı kullanılmış ve hesaplanan parametreler ile konvansiyonel parametreler arasındaki farklar belirlenmiştir. Ayrıca parametrelerin konum doğruluğuna etkisi araştırılmıştır. Stereo modelde yükseklik koh.'sı resim ölçeği, uçuş yüksekliği, baz uzunluğu ve resim koordinatlarının ölçme doğruluğuna bağlıdır. Resim koordinatları x, y nin ölçme doğruluğu da kalibrasyon doğruluğundan etkilendiği için Z değerinden bağımsız kalibrasyon alanı kullanılabilir. Arazi işleri, GPS ile üretilen ortofotoların coğrafi referans ve saha ölçümleri ve İHA'lar ile iki farklı yükseklikten çalışma alanının ölçümü. Büro çalışması, ortofotoların üretildiği, coğrafi referanslarının yapıldığı ve kontrol noktalarının GPS koordinatları ile analiz edildiği kısımdır. Elde edilen veriler ile alçak uçuş irtifasında kalibrasyonun karesel ortalama değerini düşürdüğü görülmüştür. Ancak 120 metre için benzer bir sonuç elde edilememiştir.

Anahtar kelimeler: *İHA, Fotogrametri, Kamera kalibrasyonu, Ortofoto*

1. Introduction

The effect of unmanned systems in our lives is increasing rapidly. By synchronizing itself to various disciplines, engineering science also tries to use this developing technology in accordance with its purpose of facilitating human life. One of these disciplines, aerial photogrammetry, is applicable for developing different techniques and applications with the expansion of unmanned aerial vehicles.

Aerial photogrammetry is an effective method for measuring larger areas. However, this surveying method previously made with the help of aircraft, can now be used much faster and more efficiently with the development of mini drones which help to minimize cameras in terms of their sizes.

UAVs can provide data with low-cost, high positional and temporal resolution with their GPS receivers, microprocessors, gyroscopes, sensors and communication elements, and these skills have made these systems attractive (Eisenbeiss and Sauerbier, 2011). Currently, since a simple camera, control system and a lightweight UAV are sufficient to collect photogrammetric data, these systems have begun to replace conventional systems. Compared to digital photogrammetric systems, UAV systems that can be installed at very low costs are particularly suitable for the areas with limited widths. Orthophoto, digital terrain model and topographic map production has been widely used by UAVs in recent years (Kršák et al. 2016).

Since UAVs can take images at low altitudes, they can also be used for 3D documentation of archaeological sites and structures (Mozas-Calvache et al. 2012). UAVs are also used for the following purposes: post-disaster emergency response and mapping (Li et al. 2011; Chiang et al. 2012; Zhang et al. 2018; Abdallah et al. 2019), regular measurements for monitoring environmental soil and water changes, deformation tracking (Niethammer et al. 2012), volume calculations for excavation sites and recording of natural resources, monitoring of traffic conditions (Liu et al. 2019). It is seen that it is used in many different important areas such as the documentation of traffic accidents (Pérez et al. 2019), civil infrastructure applications (Greenwood et al. 2019), agricultural applications (Song et al. 2019; Wang et al. 2019; Wu et al. 2019), coastal bathymetries (Simarro et al. 2021). They are also very practical for continuously repeatable flight and mapping studies at low costs, crop forecasting, disease detection and monitoring in the forestry and agriculture sectors (Stagakis et al. 2012), monitoring of fire zones (Krull et al. 2012). Data generation with UAV also serves to create the 3D data infrastructure required for multimedia geographic information systems. The derivation of location-based information using drones is becoming increasingly common.

One of the necessary stages of photogrammetric data processing studies is geometric camera calibration. The dynamic development of photogrammetry has led to the emergence of many calibration methods. Unfortunately, none of them make it possible to directly measure elements of internal orientation. Instead, other physical properties closely related to the determined parameters are measured. On the other hand, the determining factors of the internal orientation are the sources of error that affect the geometric accuracy of the final photogrammetric studies. Camera calibration parameters can be considered pre-calibrated and constant, or their values can be re-estimated in the self-calibrating bundle block adjustment. Various investigations have been carried out on the systematic errors in 3D measurements and strategies have been proposed for systematic error mitigation. A first focus is given to different camera calibration models. One category consists of physical models which mitigate systematic errors according to their assumed physical behavior. In the other category, individual error sources are not explicitly treated. Instead, numerical models are designed to compensate for the total systematic errors. The camera calibration can be performed with two strategies: it can either be performed independently of aerial acquisitions (pre-calibration) or be included in the bundle block adjustment (self-calibration) (Zhou et al. 2020).

In this study; the effect of position errors has been studied and analyzed in orthophoto maps which obtained from two different flight heights with refreshing camera calibration values between conventional camera calibration values for an UAV. The refreshing calibration values are calculated from PI3000 calibration software before flights. The conventional calibration values are came from the standard UAV camera calibration report which are used by the standard mapping software database. An area on the south side of Gebze Technical University Campus has been designated as a study area for this purpose. Orthophotos obtained from flight heights of 60 meters altitude and 120 meters altitude were used for the analysis by utilizing both of the calibration values. 87 points, 6 for georeferencing and 81 for comparison points have been signalized and it's RTK measurements of coordinates within two series with GPS in the orthophoto acquisition area. 6 points are used for georeferencing all orthophotos. Another 81 points were used to compare and analyze the position accuracy of the orthophotos. Thus, the accuracy of orthophotos produced by the software was analyzed only for the differences of calibration values and the accuracy of them was examined.

Flow for the preparation of this article; In the second section of this paper, information about the fundamental concepts of digital photogrammetry is given. The third part, the application of the publication is explained in detail. The fourth section the accuracy of ortho-photos obtained from images acquired by unmanned aerial vehicle are analyzed. In the fifth section, the results obtained at the end of the study are evaluated, some inferences and recommendations are made.

2. Method

Photogrammetry allows the creation of the objects without touching the objects and performs the determination of some of their properties. Photogrammetric method is to automatically connect the basic parameters of at least two different images which cover the same area. The majority of the photogrammetric process sequences are mostly related to matching.

The central perspective projection is usually preferred when performing operations on photogrammetric images. This projection system is called epipolar geometry and provides a considerable limit. When the two images considered, this plane is defined as a plane that contains the epipolar plane object point and the projection center of the two images in three-dimensional space, and it intersects two images with lines that are considered epipolar lines. For example, if the relative orientations of both images are known, the epipolar line can be calculated for the point in one image, and the corresponding point is always found on the epipolar line. So, the image matching problem turns into a one-dimensional task from a two-dimensional task.

The functional model includes the obvious characteristics of the physical condition and the stochastic model provides the probable properties. The mathematical model is a mathematical representation of the points associated with the photograph in the space coordinate system. According to the collinearity, the lights showing the points in the space coordinate system are projected from the image's projection center to the image plane. This process is done in two stages. The first stage is to determine internal orientation parameters. The second stage is to locate the external orientation parameters. The tilt of these images and the coordinates in the space coordinate system are calculated in Equation 1.

$$\begin{bmatrix} x - x_0 \\ y - y_0 \\ -c \end{bmatrix} = \frac{1}{s} . R. \begin{bmatrix} X - X_0 \\ Y - Y_0 \\ Z - Z_0 \end{bmatrix} \tag{1}$$

in equation;

x, y: Image coordinates,
x_0, y_0: Image coordinates of the projection center,
c: Camera focal length,
s: Scale factor,
R: Rotation matrix,
X, Y, Z: Object coordinates,
X_0 Y_0 Z_0 : Object coordinates of the projection center,

$$\begin{aligned} \mathrm{x} &= x_0 - \mathrm{c}\, \frac{R_{11}(\mathrm{X} - X_0) + R_{12}(\mathrm{Y} - Y_0) + R_{13}(\mathrm{Z} - Z_0)}{R_{31}(\mathrm{X} - X_0) + R_{32}(\mathrm{Y} - Y_0) + R_{33}(\mathrm{Z} - Z_0)} \\ \mathrm{y} &= y_0 - \mathrm{c}\, \frac{R_{21}(\mathrm{X} - X_0) + R_{22}(\mathrm{Y} - Y_0) + R_{23}(\mathrm{Z} - Z_0)}{R_{31}(\mathrm{X} - X_0) + R_{32}(\mathrm{Y} - Y_0) + R_{33}(\mathrm{Z} - Z_0)} \end{aligned} \tag{2}$$

The relation in Equation 2 is the relation to collinearity (linearity). The terms x_0, y_0 and c (f) in this equation represent internal orientation elements, X_0, Y_0, Z_0, and R external orientation elements. Internal orientation elements can be determined by calibration of the sensor, while external orientation elements can be determined by ground control points (GCPs) or GPS, IMU or star cameras. The rotation matrix R can also be created with angles and vectors. Image coordinates have been converted into object coordinates by equation 3. Thus;

$$\begin{aligned} \mathrm{X} &= X_0 + (Z - Z_0)\, \frac{R_{11}(\mathrm{x} - x_0) + R_{21}(y - y_0) - R_{31}c}{R_{13}(\mathrm{x} - x_0) + R_{23}(y - y_0) - R_{33}c} \\ \mathrm{Y} &= Y_0 + (Z - Z_0)\, \frac{R_{12}(\mathrm{x} - x_0) + R_{22}(y - y_0) - R_{32}c}{R_{13}(\mathrm{x} - x_0) + R_{23}(y - y_0) - R_{33}c} \end{aligned} \tag{3}$$

can be written. As it can be seen, if the Z coordinate of an object is known, its X and Y coordinates can be obtained. In order to obtain all (X, Y, Z) image coordinates, at least two photographs should be taken from different angles of the same object (Kraus, 1993). The process of finding optimum values with the hardware properties of the camera system is called camera calibration. Pinhole camera calibration was modeled and formulated by Brown (1971).

Camera calibration is intended to reproduce the geometry of rays entering the camera through the projection center at the moment of exposure. The calibration parameters of the camera are: calibrated focal length —c_k; the projection centers in relation to the pictures, determined by x_0 and y_0— image coordinates of the principal point; lens distortion: radial (K_1, K_2, K_3) and decentering (P_1 and P_2) lens distortion coefficients (Wierzbicki, 2018). For a nonmetric system to be used for measuring purposes, it is necessary to calibrate the digital camera. Many scientists have researched analytical calibration procedures. High values of distortion in non-metric digital cameras have a very negative influence on the accuracy and reliability of the determination of calibration elements. Gašparović and Gajski (2016) suggests that most of the image distortion should be removed in the first step and then the final calibration should be carried out. From the statistical indicators presented the standard deviations of the angular elements of exterior orientation on the same images are up to 2 times better in a two-step calibration. Camera calibration has traditionally been and continues to be the single most significant factor determining the accuracy potential, and to a large extent also the reliability of close-range photogrammetric measurement (Luhmann et al. 2016). Theoretically, the best calibration test field consists of multiple permanent ground control points spread throughout a large area. Indoor calibration is much easier to complete independent of weather conditions. The most commonly used chessboard-style printed calibration test fields are often used in robotics, and allow for the fast and convenient calibration of small industrial cameras (Kolecki et al. 2020) proposed a method for camera calibration consisting of a calibration test field and the relevant software.

The aim of Pérez et al. (2011) is the establishment of an efficient and accurate digital camera calibration method to be used in particular working conditions. A laboratory calibration based on a flat pattern and a field calibration were fulfilled. To carry out the calibration, photomodeler software was used in both cases. In Takahashi and Chikatsu (2015), the authors described and evaluated camera calibration techniques for UAVs using images and orientation parameters of sensor values from mobile devices. The authors executed camera calibration using a test target for evaluating sensor values measured using a mobile camera. Consequently, it is confirmed the same accuracy with normal camera calibration. The test target diemantions used are 640mm, 480mm, 20mm. In the context of UAV camera calibration, assessing the accuracy of calibration parameters computed in various image block configurations by on-the-job self-calibration is still a disputed argument. Roncella and Forlani (2021) created a series of UAV synthetic photogrammetric blocks constructed with varying terrain shape, studied area shape, block control (ground and air), strip type (longitudinal, diagonal and oblique), image observation and control data precision. Empirical airborne test flights in a calibration field have shown how block geometry influences the estimated calibration parameters and how consistent the parameters from lab calibration can be reproduced (Cramer et al. 2017). Hasheminasab et al. (2021) presents automated geometric calibration strategies for UAV-based frame and line camera systems to estimate accurate system calibration parameters without the need for ground control points or manual measurements of tie points.

In calibration, the coordinates of the object points are known and internal orientation elements are searched. Calibration is very important for the accuracy of the camera's imaging ability and all measurement procedures to be done in the image. The ideal condition is usually not achieved during image acquisition. The physical structure of the camera lenses leads to a number of effects in various parts of the image plane. The physical effects of the lenses in projection are called distortion. The cameras have two types of distortion: radial (diametrical) and tangential distortion.

Radial Distortion: This is a fundamental effect that allows the details which need to appear as a straight line in the image to be curved. This effect is a systematic function that varies at different focal lengths and different lenses. Even when all points are well focused, radial distortion distorts the entire image.

Radial distortion formula is presented in Equation 4.

$$\delta r = K_1 r^3 + K_2 r^5 + K_3 r^7 \tag{4}$$

in equation K_1 and K_2 are the distortion parameters, r is the radial distance. Equation 5 shows the components of the x and y directions within the image coordinate system with the effect of this angular change.

$$\delta rx = \delta r(x - x_0)/r \tag{5}$$

Tangential Distortion: The lenses that make up the multi-lens system used in the cameras should be located on the same direction as the centers. In cases where this condition cannot be met, a geometric displacement, called tangential distortion occurs in the image.

If tangential distortion is expressed by the intersection of the coordinate axes of the picture plane, the following are obtained Equation 6 and Equation 7:

$$\delta x = P_1(r^2 + 2(\mathrm{X} - X_0)^2) + 2P_2(\mathrm{X} - X_0)(\mathrm{y} - y_0) \tag{6}$$

$$\delta y = P_2(r^2 + 2(\mathrm{Y} - Y_0)^2) + 2P_1(\mathrm{X} - X_0)(\mathrm{y} - y_0) \tag{7}$$

P_1 and P_2 are tangential distortion parameters. x, y: image coordinates, x_0, y_0: image coordinates of the principle point (PP). UAV is an entire system consisting of three basic elements: the unmanned aerial vehicle, the command system and a communication network between them.

Height (Z) in photogrammetry is not a measurement value, it is a calculated value. In photorometry, Z value is calculated from x, y image coordinates. Therefore, the accuracy of the height (Z) value mainly depends on the accuracy of the image coordinates x, y values. Height rms. (m_Z); In a stereo model as shown in Equation (8) it depends on the picture scale (m_b), flight altitude (Z), base length (B) and the measurement accuracy parallax difference of the picture coordinates (m_{P_x}). (m_{P_x}) directly depends on the measurement accuracy of the image coordinates.

$$m_Z = m_b . \frac{Z}{B} . m_{P_x} \tag{8}$$

m_{P_x}: is the measurement accuracy in the parallax difference. As a result of the calibration, the x and y image coordinates are corrected. This affects m_{P_x}, as it affects the x and y coordinates. Since the measurement accuracy of the image coordinates x, y is also affected by the calibration accuracy, the calibration field independent of the Z value can be used. Based on this idea, this study was tested.

The correction brought to the focal length c as a result of the calibration directly affects the picture scale. A change in scale, on the other hand, changes the rms of all x, y. The difference in Z values of the terrain points has no direct effect on the stochastic model of the calibration. The values corrected by the camera calibration are the corrections to the x, y values, which are the picture coordinates. As a result, the correction values in the x, y values already directly affect the accuracy in the Z value.

3. Application

The basic equipment used in the study is an unmanned aerial vehicle. Manufacturers of unmanned aerial vehicles, which have recently been used for civilian purposes, perform purpose-specific productions. Detection of maximum flight height, camera features and the most suitable hardware can be done depending on the problem by the manufacturers who offer various solutions. The purpose of this study is to investigate and analyze the effect of coordinate positioning for orthophoto maps obtained from two different flight heights with refreshing camera calibration between conventional camera calibration data for an unmanned aerial vehicle has been studied and analyzed. The refreshing camera calibration values obtained from PI3000 calibration software in planar calibration fieald before flights. Two orthophotos obtained from each flight height (60 meters altitude and 120 meters altitude) were used for the analysis by utilizing both of the refreshing and conventional camera calibration values. Figure 1. shows the flowchart that explains the process step of the study.

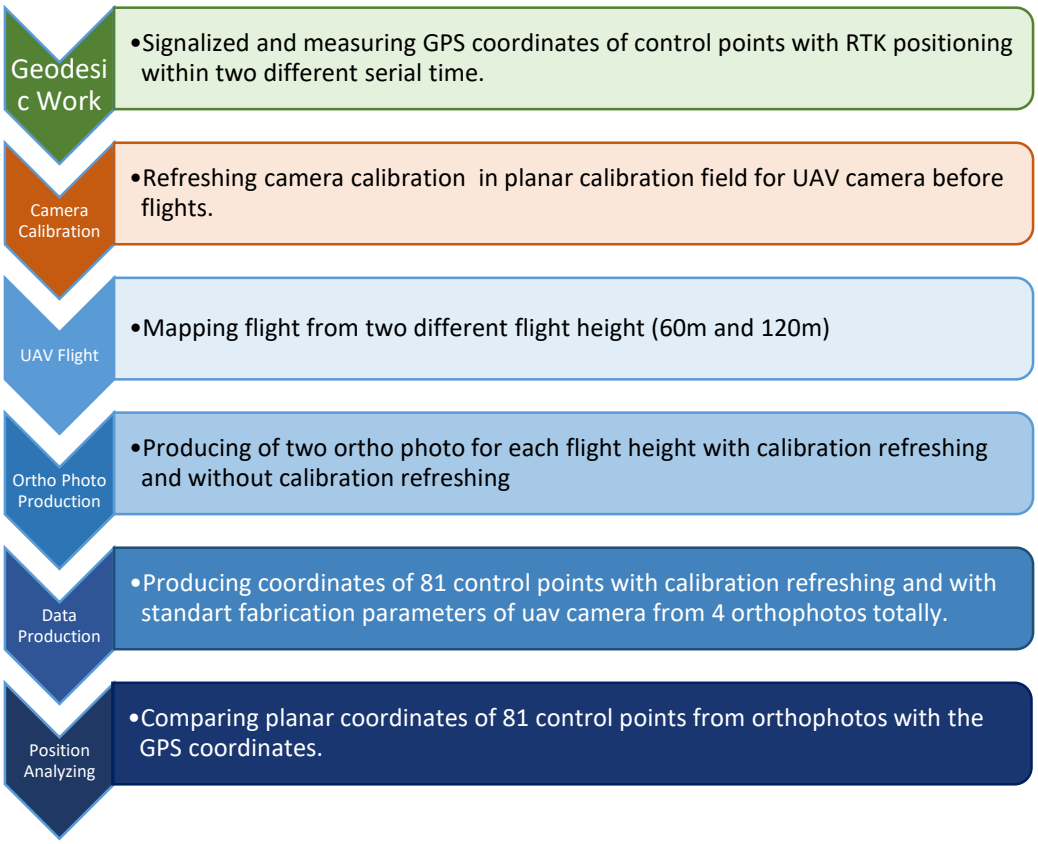

Figure 1. Flowchart of the study

Study area covers some part of the area on the south side of Gebze Technical University Campus. An area of approximately 15 hectares is decided as the study area which has shown in Figure 2.

Figure 2. Study area in Gebze Technical University Campus

The preferred unmanned aerial vehicle is In summary, while recalibrating at 60 meters flight altitude with the data obtained in the study reduces the square mean value, the calibration process at 120 meters flight altitude does not have a significant effect on the accuracy values for this study. This drone which is 1380 gram has four propellers. The camera, which is connected to the body with an integrated gimbal, has a resolution of 12 Megapixels. DJI Phantom, which can stay in the air for 28 minutes, can speed up 20 meters in 4 seconds. The hardware, which is operated with lithium batteries, has four sensors. These sensors prevent a possible collision. It provides an advantage in terms of flight safety compared to its counterparts. Table 1 illustrates technical specifications of DJI Phantom 4 Pro and Table 2 presents technical specifications of the camera equipment used in DJI Phantom 4 unmanned aerial vehicle.

Table 1. Technical specifications of DJI Phantom 4 Pro UAV

Weight	1380 gr.
Maximum Lift-off Rate	6 m/s.
Maximum Descent Rate	4 m/s.
Maximum Rate	20 m/s.
Maximum Height	6000 m.
Maximum Flight Duration	28 minutes
Satellite System	GPS/GLONASS

Table 2. Technical specifications of the camera of DJI Phantom 4 aerial vehicle

Sensor	1/2.3'' Effective Pixel
Lens	f/2.8
ISO Range	100 - 1600 (photograph)
Electronic Shutter Speed	8 s to 1/8000 s
Maximum Image Size	4000×3000
Photograph	JPEG, DNG (RAW)

Geo-referencing of orthophotos produced by UAV photogrammetry and geodesic land work was carried out in order to investigate point position accuracy between different flight-height and refreshing camera calibration parameters and conventional camera calibration parameters.

In geodesic work, the control points required for geo-referencing and analysis of the point accuracy. The clear and sharp detail points to in the photographs taken by the UAV were determined as the control points. These points were measured with the GNSS device. The measuring process of ground control points was made with the Leica Viva GS15 GNSS device and the coordinates were obtained in 2005.00 EPOK in the ITRF96 datum system. For this purpose, measurements were made in two different time periods. Three minutes of measurement was made at each control point. Coordinates which were provided by two different series were averaged. In the study, an accuracy study is carried out based on geodesic coordinates from the GPS measurement within RTK method. After measuring the control points, photographs of the study area were taken with the UAV.

As it is illustrated in Figure 4, the calibration images from 5 different projection points of the planar calibration area of PI-3000 software with the DJI Phantom 4 Pro standard camera are used for calibration in PI-3000 software and the values obtained as a result of calibration are combined for the purpose of production of orthophotos as a refreshing camera calibration parameters. The calibration page used to determine the projection parameters and distortion function of the camera is in Figure 3.

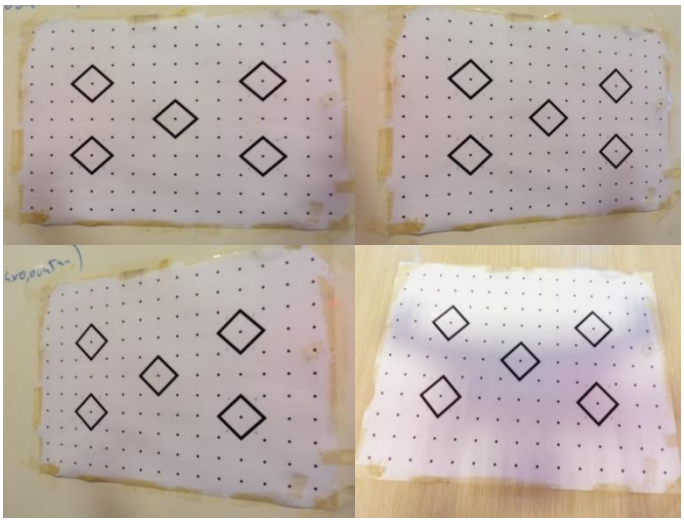

Figure 3. Calibration sheet and angles of photography

Orthophotos produced with calibration values obtained using PI3000 software are called orthophotos produced with calculated parameters. Figure 4 shows calibration results for image distortion in PI3000 software. Orthophotos produced with different calibration values obtained by flights of the same height will offer the possibility to compare the values. Both of the calibration values which used in the study have been presented in Table 3.

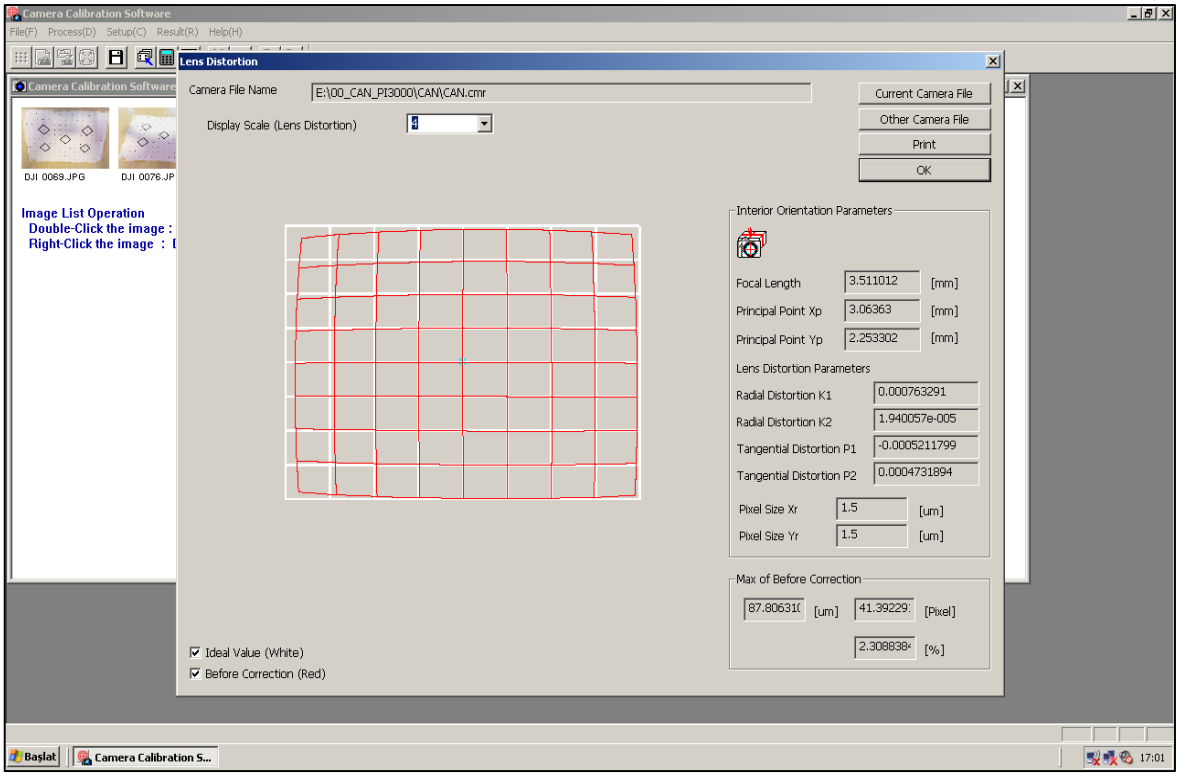

Figure 4. DJI Phantom 4 PRO camera calibration in PI3000 software

Table 3. Normal/Parameterized calibration values

Camera	c (mm)	x_0 (mm)	y_0 (mm)	k_1	k_2	p_1	p_2
Conventional (Standard)	3.61000	3.15875	2.36906	-0.001358	-0.001605	-0.000909	-0.001138
Calibration (Refreshing)	3.51101	3.06364	2.25330	0.000763	0.000019	-0.000521	0.000473

The imaging study was performed with the standard digital camera integrated into the DJI Phantom 4 Pro UAV system in Figure 5.

Information such as flight height, horizontal and vertical speed could be read on the display of the image transfer system and photographs from two different heights were taken with UAV's GPS mode (60 m altitude and 120 m altitude). During imaging section, overlay rates were 70% transverse and 80% longitudinal.

Figure 5. DJI Phantom 4 pro drone set

For covering the study area; a total of 307 images from a flying height of 60 meters and 112 images from a height of 120 meters were acquired. Figure 6 has shown the flight line and the points of imaging from a height of 60 meters. Figure 7 has shown the flight line and the points of imaging from a height of 120 meters.

Figure 6. Imaging Plan for flying height of 60 meters altitude

Figure 7. Imaging Plan for flying height of 120 meters

The normal parameters which are automatically calculated by the orientation parameters owned by the camera and shown in the PIX4D software integrated on DJI Phantom 4 PRO, are used without making any changes. Orthophotos produced with these calibration parameters are denominated with the names which correspond to the calculation made by normal parameters. Images have been automatically matched after flights from 60 m and 120 m altitudes, the default internal and external orientation parameters are used, and they are installed into the PIX4D software. 81 points are used as the ground control points for comparison in the final stage of the study. This process is only functional to control data which occur as a result of different flights and refreshing camera parameters.

The stages of orthophoto production in PIX4D are as follows. First, aerial images are uploaded to the program. The projection system and earth zone of the project are introduced to the program. This process is intended to transform geographic coordinates. Ground control points are added to the program and the image coordinates of the control points on the images are measured.

This process is done separately with conventional calibration parameters for 60 meters altitude and 120 meter altitude flights. Additionally, with refreshing camera parameters from the PI3000 software, orthophotos for 60 meters altitude and 120 meters altitude are also produced.

As a result of all this study, 4 orthophotos were produced. 2 out of 4 orthophotos which were produced with refreshing camera calibration parameters (for 60 meters and 120 meters) are shown in Figure 8 and Figure 9.

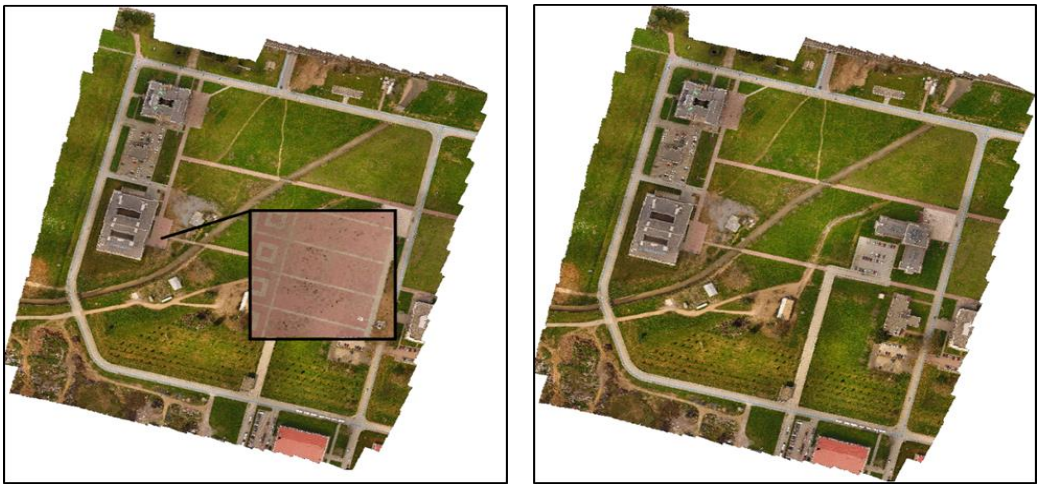

(a) Without Refreshing for calibration (b) Refreshing for Calibration

Figure 8. Orthophotos obtained from the flight height of 60 meters altitude with normal and parameterized calibration values

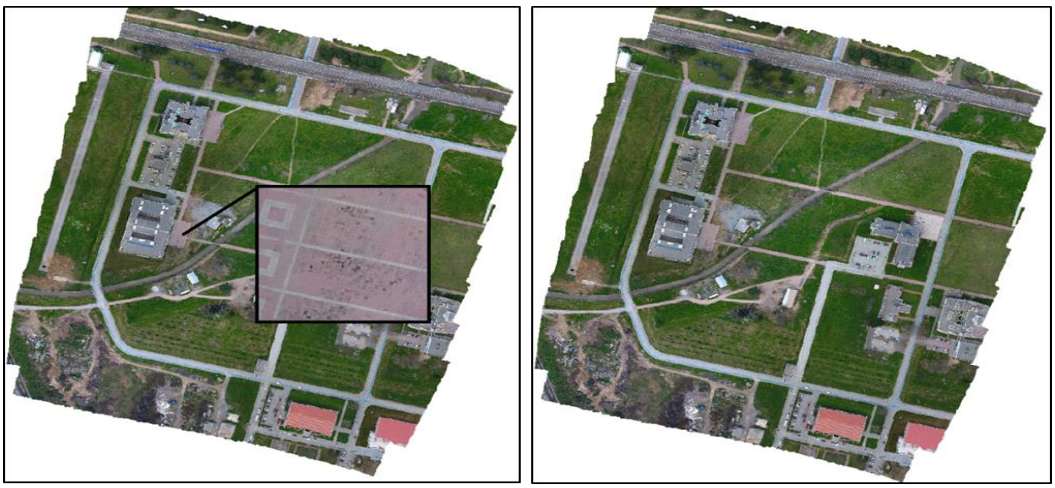

(a) Without Refreshing for calibration (b) Refreshing for Calibration

Figure 9. Orthophotos obtained from the flight height of 120 meters altitude with normal and parameterized calibration values

4. Result and Analysis

Error vectors between coordinates which are considered conventional camera calibration between refreshing camera parameters, obtained as a result of geodesic measurement with control point coordinates read from the orthophoto obtained using images from flight height of 60 meters altitude and conventional calibration parameters are shown in Figure 10 and Figure 11. When Figure 10 and Figure 11 are compared, the control points above the building have a higher standard deviation than the points on the ground. In addition, the accuracy of the ground control points towards the center of the study area increases.

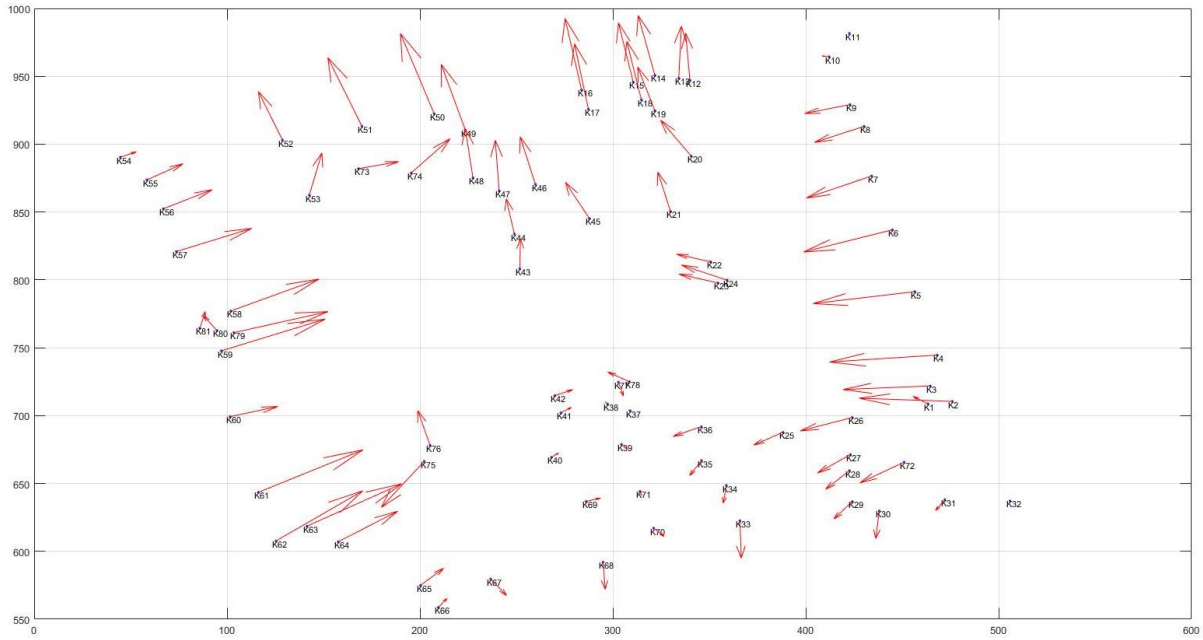

Figure 10. Point position vectors between a normal parameter orthophoto and ground control points (GPS) produced from a height of 60 meters altitude

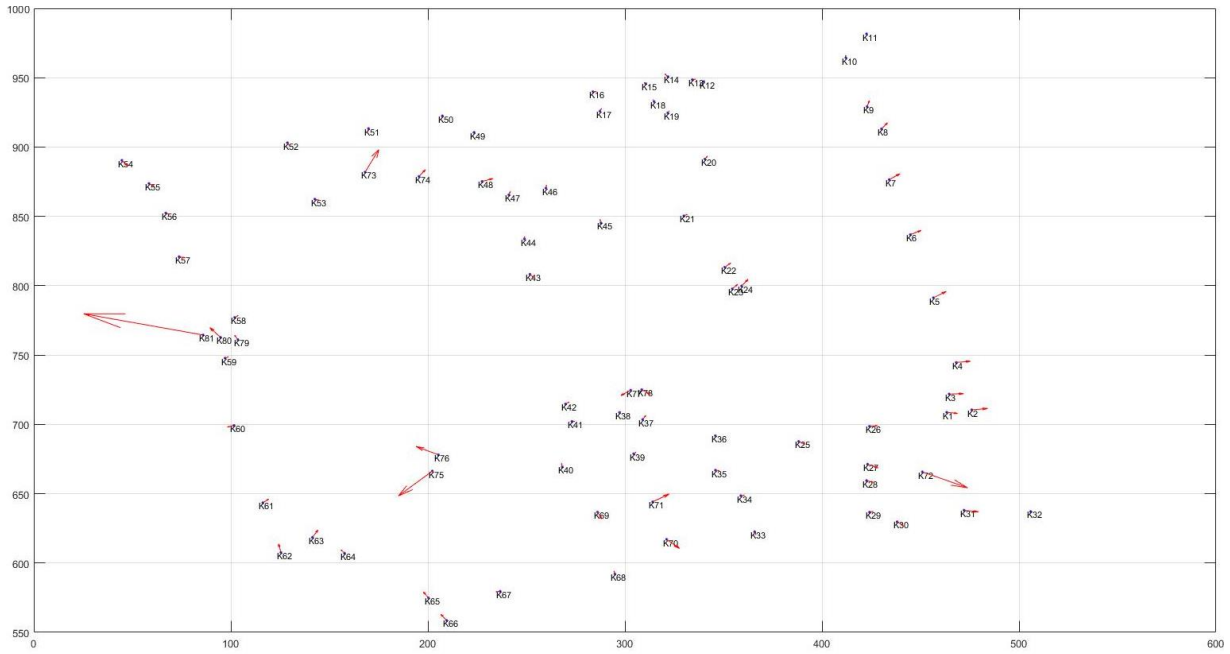

Figure 11. Point position vectors between a calibrated parameter orthophoto and ground control points (GPS) produced from a height of 60 meters altitude

Error vectors between coordinates which are considered conventional camera calibration between refreshing camera parameters, obtained as a result of geodesic measurement with control point coordinates read from the orthophoto obtained using images from flight height of 120 meters altitude and conventional calibration parameters are shown in Figure 12 and figure 13.

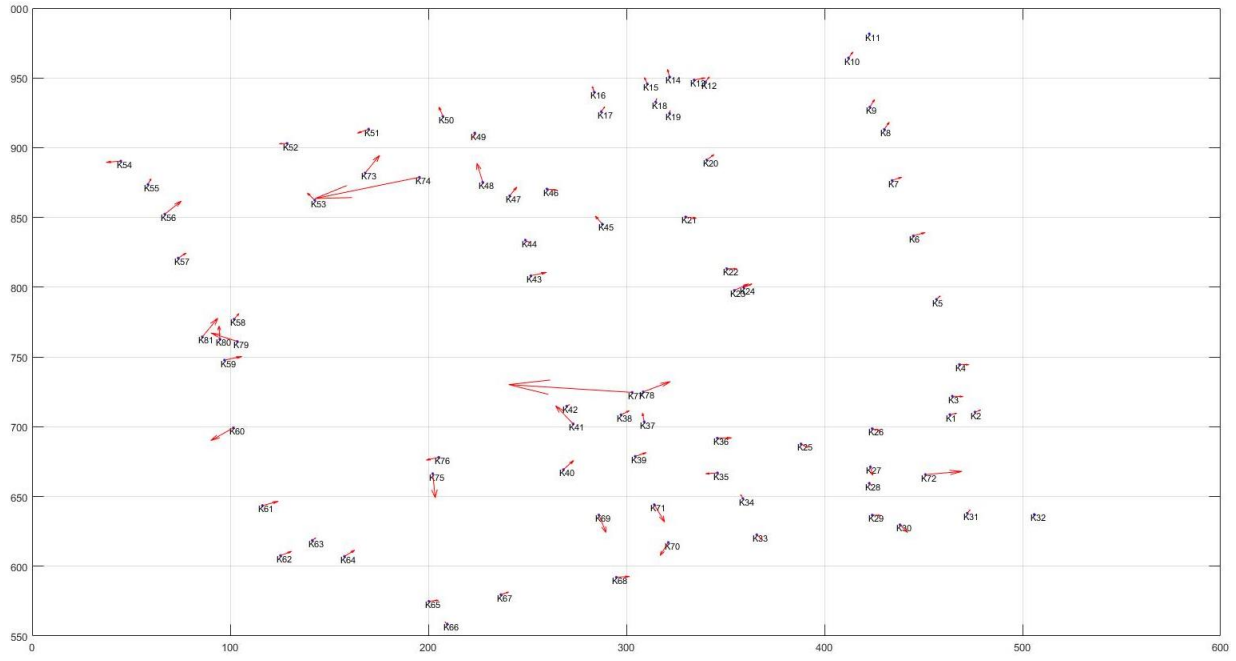

Figure 12. Point position vectors between a normal parameter orthophoto and ground control points (GPS) produced from a height of 120 meters altitude

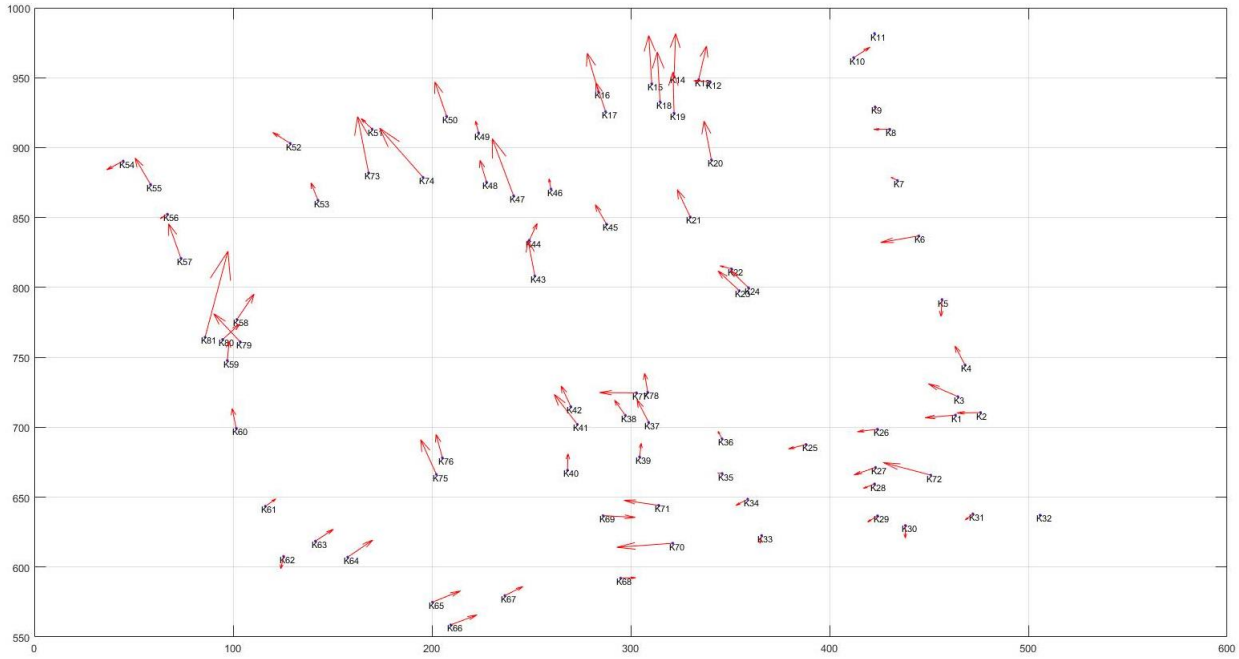

Figure 13. Point position vectors between a calibrated parameter orthophoto and ground control points (GPS) produced from a height of 120 meters altitude

According to results, which focuses on investigating and analyzing the differences for coordinates between orthophotos obtained by flights from altitudes of 60 m and 120m. Stabilizing the observation area, the hardware and software features is important for determining the sensitivity differences in area-sample ranges at different heights.

In addition, the use of different flight heights and calibration parameters and its effects on X and Y position accuracies are shown. It is shown that the standard deviation of the results decreases. It is also thought that coarse errors usually occur when the operator evaluation is performed. Analysis is done in Table 4 for X and Y axes because there are high area errors on building roofs and established control points which are at a different height than the ground level. The differences are obvious. As the height of the control points in the study area increases, there is also an increase in standard deviation. The chart in Table 4 is presented in Figure 14 and Figure 15.

Table 4. Standard deviation table

Position RMS	60m Conventional	60m Refreshing	120m Conventional	120m Refreshing
Std X (m)	0,035389685	0,033469707	0,022534359	0,037740845
Std Y (m)	0,057888305	0,055663007	0,048610602	0,058657069

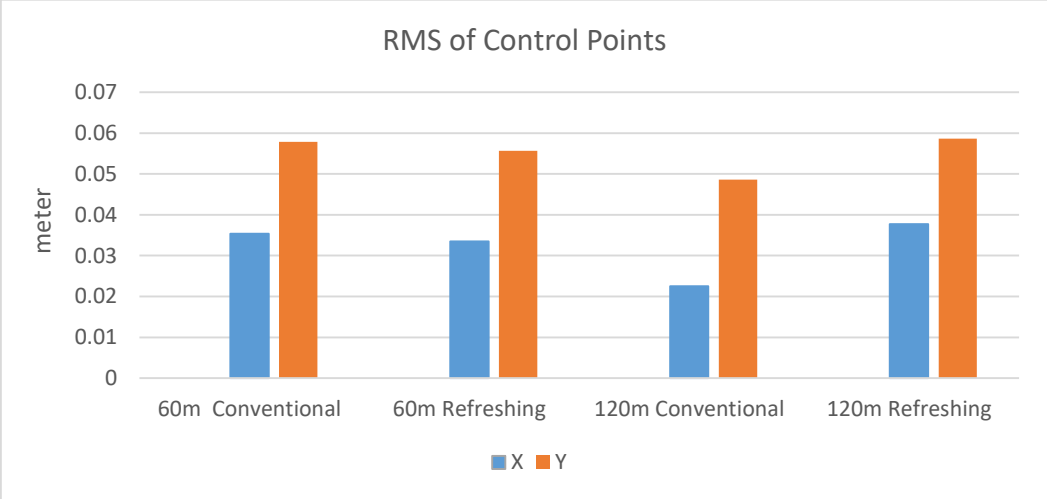

Figure 14. Standard deviation

When the above charts and analyses are examined;

The results of the course incorrect points and the control points marked above the building are shown in the tables above. When these tables are examined, the standard deviation of the "Y" axis coordinates is greater than the "X" axis coordinates. Although the position accuracy of X's is higher, it varies depending on the flight direction (Table 4).

When examining standard deviation graphs from flights of 60 and 120 meters, a flight height of 120 meters indicates that the camera gives better results than other samplings (Figure 14).

Between orthophotos made with both normal and calibration of flights made of 60 meters altitude, the position accuracy ratio of the ortho-photo with normal values is higher than the calculated orthophoto parameter. In both cases, the standard deviation of the "Y" coordinate is higher than the "X" coordinate (Figure 14).

In the comparison obtained from orthophoto, which is created with images taken from 120 meters altitude, the most accurate measurement is obtained at this height compared to others in the controls which are made using both normal and calibration parameter. A standard deviation from 0.035 m. to 0.033 m. is observed at the "X" coordinates, while the "Y" coordinates differ between 0.057 m. and 0.055 m. (Figure 14).

As a result of balancing the photos obtained with normal parameters with flights at a height of 120 m, both "X" and "Y" standard deviations are between 0.05 m. and 0.07 m. and they are in their closest position to each other. The closest accurate sample in this study is the sample made at a flight height of 120 m. for conventional values (Figure 14). The evaluation of the images taken from 120 m with the refreshing calibration parameters, It has seen that the "X" increases from 0.022 m. to 0.037 m. Also, the standard deviation of "Y" increases from 0.0048 m. to 0.058 m. As a result of all these analyses, it is interpreted that having a standard error in the "Y" coordinates or containing more errors than "X" may be caused by an axis error. Refreshing 60 meters gives the result we expect. Refreshing at 120 meters does not give the expected result. As the flight altitude increases, the calibration process does not have a significant effect on the accuracy values.

5. Conclusion

The use of unmanned systems as a measuring tool, which are widely used today and are going to be used in many disciplines brings forward many issues. The most important of these is positional accuracy and precision. In this study, using normal and calculated calibration parameters for heights of 60 meters altitude and 120 meters altitude, positional accuracy and standard deviations are tested and analyzed for different situations and conditions. 81 points were installed on the test area of the study. Of these, 45 are located on the surface and 36 are located on the roofs and terraces of the buildings. Ground control points are measured with a GPS measurement. Calibration parameters were calculated with the use of the program called PI 3000. Aerial photos were taken by DJI Phantom 4 Pro Unmanned Aerial Vehicle (UAV). Resolution of its camera was 12 MP. Orthophoto production was obtained by a commercial software called PIX4D within geo-referencing. The ground sample range of orthophoto obtained from an elevation of 60 m is 2.62 cm and has a flight length of 6000 m. It includes 307 aerial images. Because the overlay rate is constant, the number of images is higher compared to 120 m. The ground sample range of orthophoto obtained from an elevation of 120 m is 5.25 cm and has a flight length of 3200 m. A total of 112 images were taken at this height and the orthophoto has been obtained.

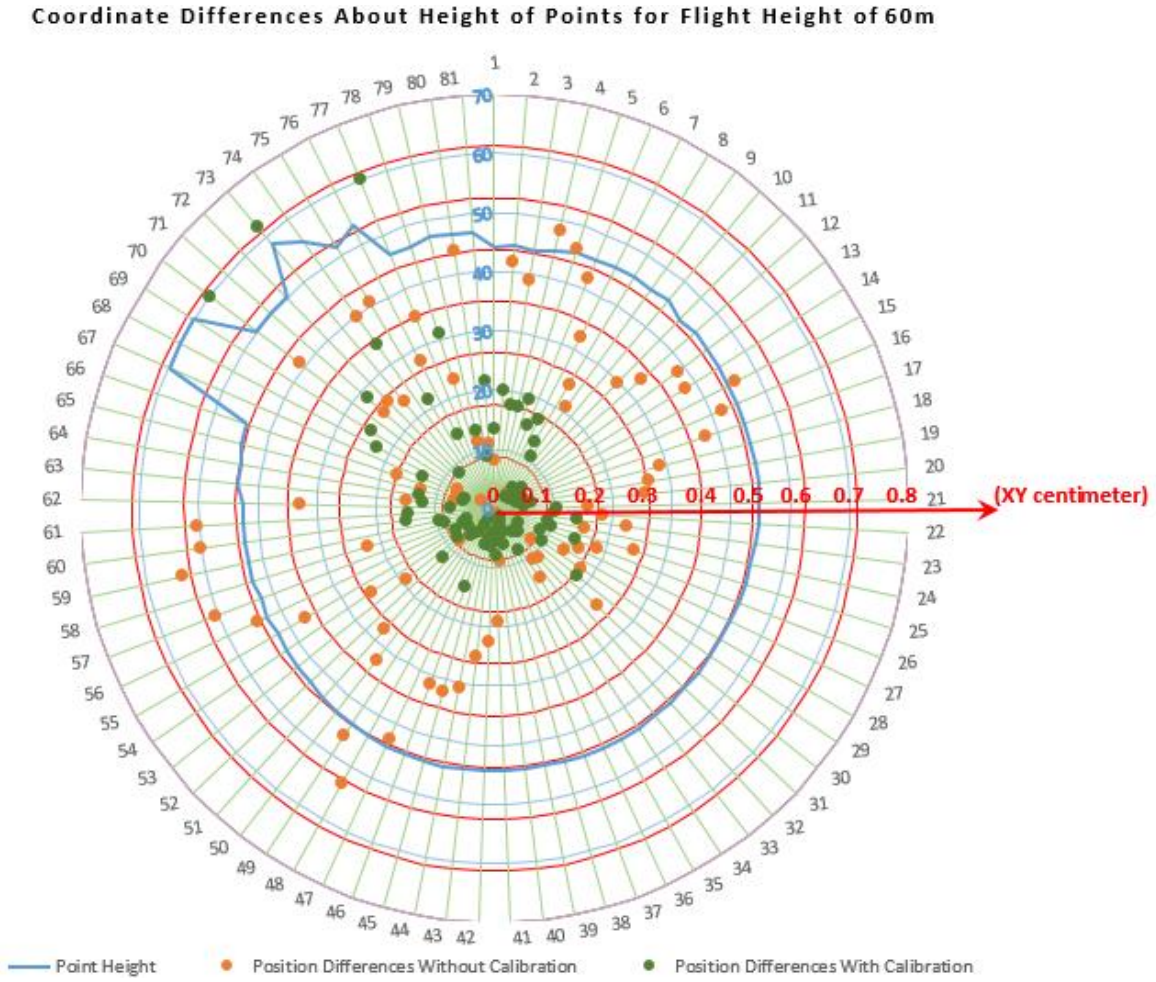

Figure 15. Coordinate differences about height of point for flight height of 60 meters altitude

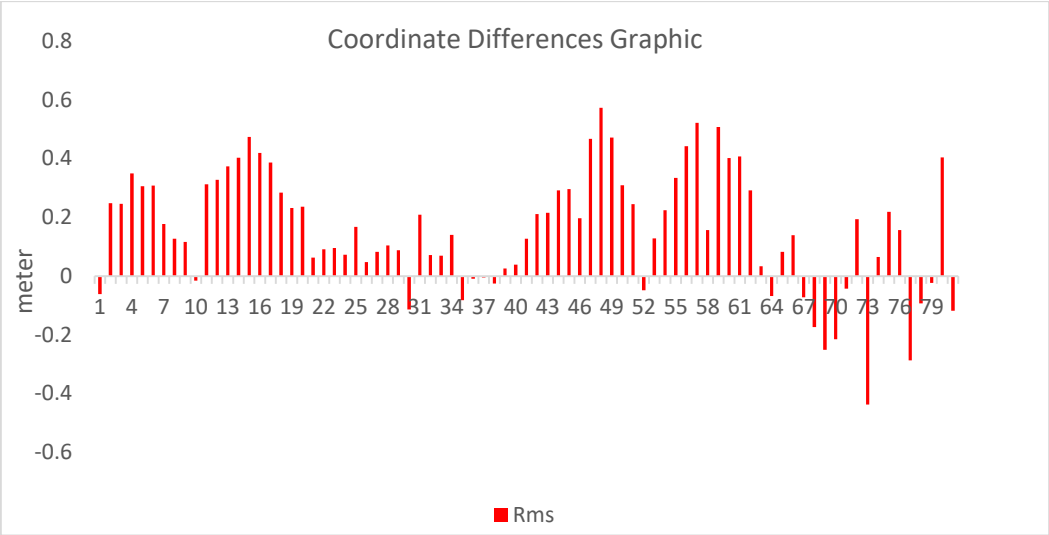

Figure 16. Coordinate differences graphic for 60 meters altitude

When Figure 15 and Figure16 are examined, it is observed that the control points in orthophotos obtained from the flight from 60 meters have lower positional differences when compared with geodesic coordinates. Especially at points where the control points used on the land shows sudden changes of height, it is seen that calibration renewal provides a significant benefit. Based on the overall height profile of the land, it can be said that the positional values of all points improve. In terms of point positional differences, positional differences are clustered in near-zero areas in this low-distance flight.

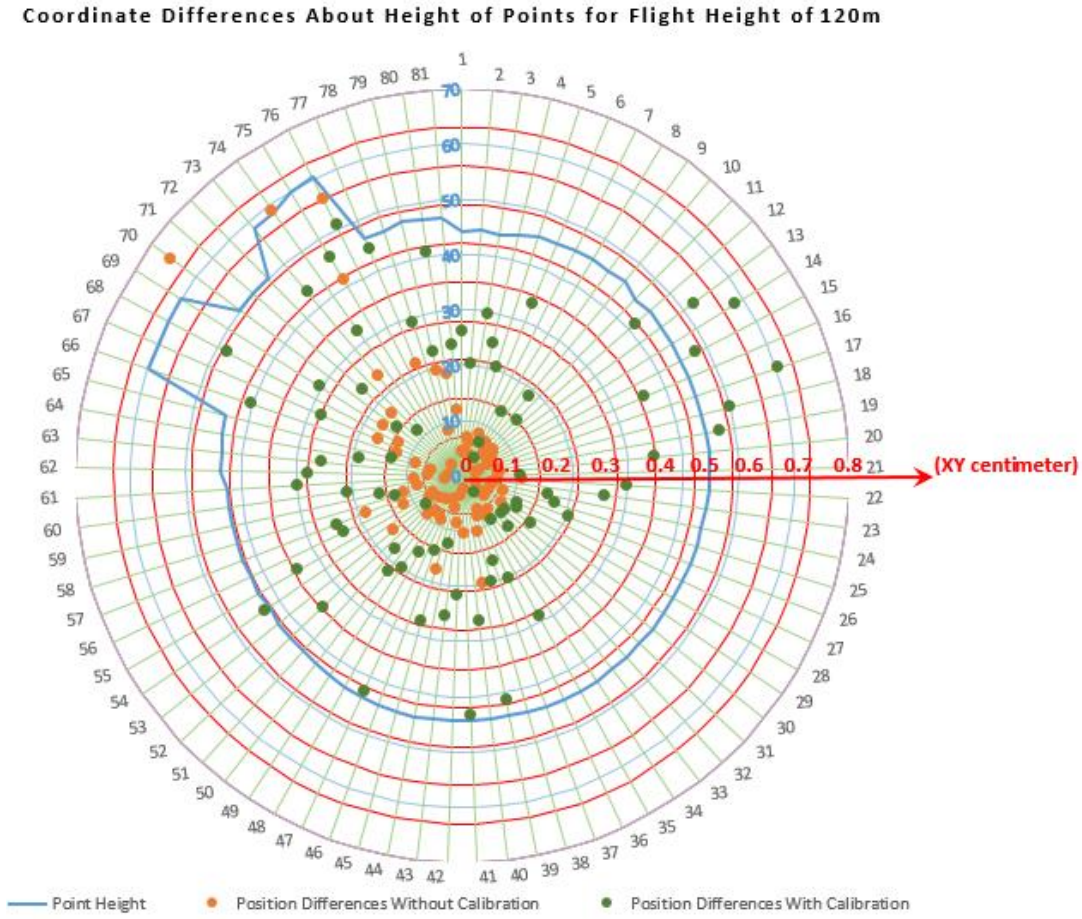

Figure 17. Coordinate differences about height of point for flight height of 120 meters altitude

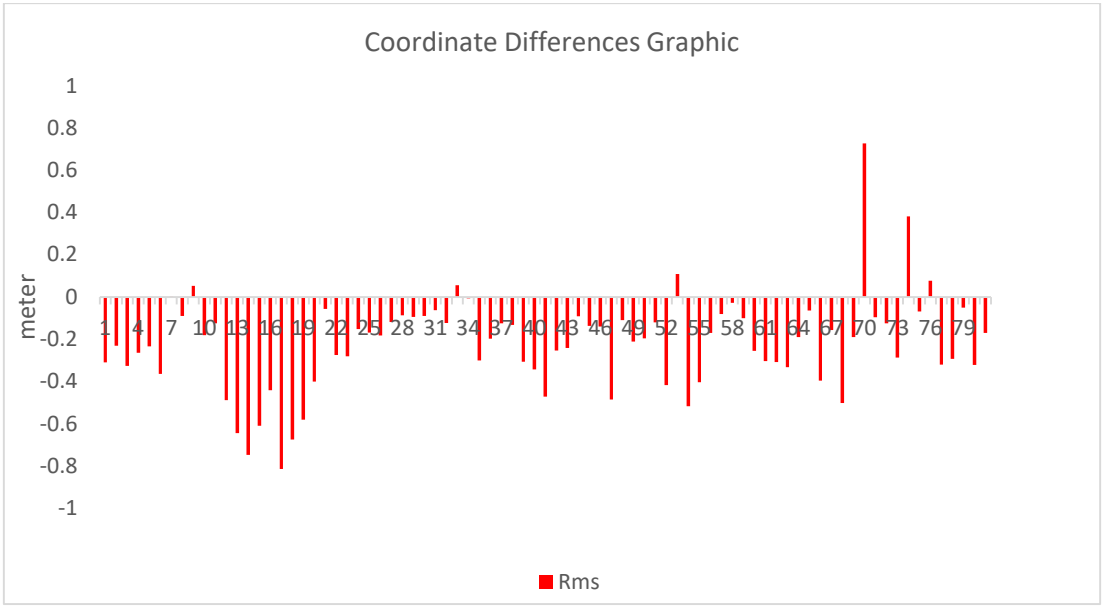

Figure 18. Coordinate differences graphic for 120 meters altitude

When Figure 17 and Figure 18 are examined, it is observed that the control points in orthophotos obtained from the flight from 120 meters have higher positional differences when compared with geodesic coordinates. Especially at points where the control points used on the land shows sudden changes of height, it is seen that calibration renewal provides a limited benefit. These renewed calibration values and distortion parameters must be used in place of default software calibration values in low distance flight orientations.

In the literature, there are studies focused on the field calibration method. Pérez et al. (2011) presents a study comparing laboratory and field calibration. In labarator calibration, the images covered the calibration grid pattern included in package of Photomodeler. The grid pattern was placed on the floor and three images were collected from each of the pattern´s four sides. The field test used in the study was a flat surface located and a set of 67 target points were placed. The calibration field area was 25 x 25 m approximately and the altitude flight over ground was 50 m. The laborator calibration has a final total error of 1.940 pixels. The field calibration has a total error of 0.282 pixels. Field calibration method reduced the final total error obtained in the previous laboratory calibration. Furthermore the overall rms obtained from both methods are similar. In this study, the default calibration parameter of the DJI Phantom 4 Pro and the calibration parameters obtained from the PI3000 software were examined. In summary, while recalibrating at 60 meters flight altitude with the data obtained in the study reduces the square mean value, the calibration process at 120 meters flight altitude does not have a significant effect on the accuracy values.

References

Abdallah, A., Ali, M. Z., Misic, J., & Misic, V. (2019). Efficient security scheme for disaster surveillance UAV communication networks. *Information, 10*(2), 43. doi: 10.3390/info10020043.

Brown, D. C. (1971). Close-range camera calibration. *Photogrammetric Engineering, 37*(8), 855-866.

Chiang, K. W., Tsai M. L., & Chu C. H. (2012). The development of an UAV borne direct georeferenced photogrammetric platform for ground control point free applications. *Sensors, 12*(7), 9161-9180.

Cramer, M., Przybilla, H. J., & Zurhorst, A. (2017, September). UAV Cameras: overview and geometric calibration benchmark. In *International Conference on Unmanned Aerial Vehicles in Geomatics, 2017*. *Proceedings*. (pp. 85-92). ISPRS.

Eisenbeiss, H., & Sauerbier, M. (2011). Investigation of UAV systems and flight modes for photogrammetric applications. *Photogrammetric Record, 26*(136), 400-421.

Gašparović, M., & Gajski, D. (2016, July). Two-step camera calibration method developed for micro UAV's. In *XXIII ISPRS Congress, 2016. Proceedings*. (pp. 829-833). ISPRS.

Greenwood, W. W., Lynch J. P., & Zekkos D. (2019). Applications of UAVs in civil infrastructure. *Journal of Infrastructure Systems, 25*(2), 9-15.

Hasheminasab, S. M. Zhou, T., LaForest, L. M., & Habib, A. (2021). Multiscale image matching for automated calibration of UAV-based frame and line camera systems. *IEEE Journal of Selected Topics in Applied Earth Observations and Remote Sensing, 14*, 3133-3150.

Kolecki, J., Kuras, P., Pastucha, E., Pyka, K., & Sierka, M. (2020). Calibration of industrial cameras for aerial photogrammetric mapping. *Remote Sensing, 12*(19), 3130. doi:10.3390/rs12193130.

Kraus, K. (1993). *Photogrammetry, Vol. 1: Fundamentals and Standard Processes*. Bonn, Germany: Dümmlers.

Kršák, B., Blištan, P., Pauliková, A., Puškárová, P., Kovanic, L., Palková J., & Zeliznaková, V. (2016). Use of low-cost UAV photogrammetry to analyze the accuracy of a digital elevation model in a case study. *Measurement, 91*, 276-287.

Krull, W., Tobera, R., Willms, I., Essen, H., & Wahl, N. (2012). Early forest fire detection and verification using optical smoke, gas and microwave sensors. *Procedia Engineering, 45*, 584-594.

Li, C. C., Zhang, G. S., Lei, T. J., & Gong, A. (2011). Quick imageprocessing method of UAV without control points data in earthquake disaster area. *Transactions of Nonferrous Metals Society of China, 21*(3), 523-528.

Liu, X. F., Peng, Z. R., & Zhang L.Y. (2019). Real-time UAV rerouting for traffic monitoring with decomposition based multi-objective optimization. *Journal of Intelligent & Robotic Systems, 94*(2), 491-501.

Luhmann, T., Fraser, C., & Maas, H. G. (2016). Sensor modelling and camera calibration for close-range Photogrammetry. *ISPRS Journal of Photogrammetry and Remote Sensing, 115*, 37-46.

Mozas-Calvache, A. T., Perez-Garcia, J. L., Cardenal-Escarcena, F. J., Mata-Castro, E., & Delgado-Garcia, J. (2012). Method for photogrammetric surveying of archaeological sites with light aerial platforms. *Journal of Archaeological Science, 39*(2), 521-530.

Niethammer, U., James, M. R., Rothmund, S., Travelletti, J., & Joswig, M. M. (2012). UAV-based remote sensing of the super-sauze landslide: Evaluation and results. *Engineering Geology, 128*, 2-11.

Pérez, J. A., Goncalves G. R., Rangel, J. M. G., & Ortega P. F. (2019). Accuracy and effectiveness of orthophotos obtained from low cost UASs video imagery for traffic accident scenes documentation. *Advences in Engineering Software, 132*, 47-54.

Pérez, M., Agüera, F., & Carvajal, F. (2011, September). Digital camera calibration using images taken from an unmanned aerial vehicle. In *ISPRS Zurich 2011 Workshop, 2011. Proceedings*. (pp. 167-171). ISPRS.

Roncella, R., & Forlani, G. (2021). UAV block geometry design and camera calibration: A simulation study. *Sensors, 21*(18), 6090. doi:10.3390/s21186090.

Simarro, G., Calvete, D., Plomaritis, T.A., Moreno-Noguer, F., Giannoukakou-Leontsini, I., Montes, J., & Durán, R. (2021). The influence of camera calibration on nearshore bathymetry estimation from UAV videos. *Remote Sensing, 13*(1), 150. doi: 10.3390/rs13010150.

Song, F., Dan, T., Yu, R., Yang, K., Yang, Y., Chen W. Y., Gao, X. Y., & Ong, S. H. (2019). Small UAV-based multi-temporal change detection for monitoring cultivated land cover changes in mountainous terrain. *Remote Sensing Letters, 10*(6), 575-581.

Stagakis, S., Gonzalez-Dugo, V., Cid, P., Gullien, M. L., & Zarco-Tejoda, P. J. (2012). Monitoring water stress and fruit quality in an orange orchard under regulated deficit irrigation using narrow-band structural and physiological remote sensing indices. *ISPRS Journal of Photogrammetry and Remote Sensing, 71*(2012), 47-61.

Takahashi, Y., & Chikatsu, H. (2015, May). Camera calibration for UAV application using sensor of mobile camera. In *Indoor-Outdoor Seamless Modelling, Mapping and Navigation, 2015. Proceedings*. (pp. 239-242). ISPRS.

Wang, F. L., Wang, F. M., Zhang, Y., Hu, J. H., Huang, J. F., & Xie, J. K. (2019). Rice yield estimation using parcel-level relative spectra variables from UAV-based hyperspectral imagery. *Frontiers Plant Science, 10*, 453. doi:10.3389/fpls.2019.00453.

Wierzbicki, D. (2018). Multi-camera imaging system for UAV photogrammetry. *Sensors, 18*(8), 2433. doi:10.3390/s18082433.

Wu, Z. C., Ni, M., Hu, Z. W., Wang, J. J., Li, Q. Q., & Wu, G. F. (2019). Mapping invasive plant with UAV-derived 3D mesh model in mountain area-A case study in Shenzhen Coast, China. *International Journal of Applied Earth Observation and Geoinformation, 77*, 129-139.

Zhang, N., Zhang, X. L., Yang, G. J., Zhu, C. H., Huo, L. N., & Feng, H. K. (2018). Assessment of defoliation during the Dendrolimus tabulaeformis Tsai et Liu disaster outbreak using UAV-based hyperspectral images. *Remote Sensing of Enviroment, 217*, 325-337.

Zhou, Y., Rupnik, E., Meynard, C., Thom, C., & Pierrot-Deseilligny, M. (2020). Simulation and analysis of photogrammetric UAV image blocks-influence of camera calibration error. *Remote Sensing, 12*(1), 22. doi:10.3390/rs12010022.